

Article

Not peer-reviewed version

---

# Optimized Open-Source Setting for Subjecting Rodents to Chronic Normobaric Hypoxia in Facilities with Minimal Nitrogen Supply

---

[Jorge Otero](#) \* , Miguel A. Rodriguez-Lazaro , Raffaella Salama , Daniel Mbanze , Gorka Solana ,  
Vincent Muñoz-Vaño , Yolanda Camara , [Isaac Almendros](#) , [Ramon Farre](#) \*

Posted Date: 8 December 2025

doi: 10.20944/preprints202512.0632.v1

Keywords: oxygen sensor; animal research; gas concentration control; CO<sub>2</sub> monitoring; hypoxia model



Preprints.org is a free multidisciplinary platform providing preprint service that is dedicated to making early versions of research outputs permanently available and citable. Preprints posted at Preprints.org appear in Web of Science, Crossref, Google Scholar, Scilit, Europe PMC.

Copyright: This open access article is published under a [Creative Commons CC BY 4.0 license](#), which permit the free download, distribution, and reuse, provided that the author and preprint are cited in any reuse.

Disclaimer/Publisher's Note: The statements, opinions, and data contained in all publications are solely those of the individual author(s) and contributor(s) and not of MDPI and/or the editor(s). MDPI and/or the editor(s) disclaim responsibility for any injury to people or property resulting from any ideas, methods, instructions, or products referred to in the content.

Article

# Optimized Open-Source Setting for Subjecting Rodents to Chronic Normobaric Hypoxia in Facilities with Minimal Nitrogen Supply

Jorge Otero <sup>1,2,\*</sup>, Miguel A. Rodríguez-Lázaro <sup>1</sup>, Raffaella Salama <sup>1</sup>, Daniel Mbanze <sup>1,3</sup>, Gorka Solana <sup>3</sup>, Vicent Muñoz-Vaño <sup>4</sup>, Yolanda Cámara <sup>4,5</sup>, Isaac Almendros <sup>1,2</sup> and Ramon Farré <sup>1,2,\*</sup>

<sup>1</sup> Unit of Biophysics and Bioengineering, School of Medicine and Health Sciences, University of Barcelona. Casanova 143, 08036 Barcelona, Spain

<sup>2</sup> CIBER of Respiratory Diseases (CIBERES), Monforte de Lemos 3-5, 28029 Madrid, Spain

<sup>3</sup> Faculdade de Engenharias e Tecnologias, Universidade Save. Av. Américo Boavida s/n, Maxixe, Inhambane, Mozambique

<sup>4</sup> Vall d'Hebron Research Institute (VHIR) Passeig Vall d'Hebron 119-129, 08035 Barcelona, Spain

<sup>5</sup> CIBER of Rare Diseases (CIBERER), Monforte de Lemos 3-5, 28029 Madrid, Spain

\* Correspondence: jorge.otoero@ub.edu (J.O.); rfarre@ub.edu (R.F.)

## Abstract

Very prevalent respiratory and cardiovascular diseases result in chronic hypoxia, promoting metabolic, kidney, heart, and other malignant diseases. Hypoxia research employs animal models based on chronically breathing hypoxic air ( $O_2 < 21\%$ ), usually by injecting  $N_2$  into the animal's chamber. However, continuous high-flow  $N_2$  supply is available only in limited facilities, reducing the capability of widely conducting hypoxia research. Here, we describe an optimized setting for subjecting rodents to chronic normobaric hypoxia by requiring minimal  $N_2$  supply. The setting is based on providing the  $O_2$  consumed by the animals and eliminating the exhaled  $CO_2$  and water vapor.  $O_2$ ,  $CO_2$ , temperature, and humidity in the hypoxic chamber are controlled by an Arduino-based unit activating a pump that introduces room air to restore the metabolized  $O_2$ . Another pump continuously recirculates the chamber air through a Peltier-based dryer and  $CO_2$ -absorbing soda lime. To correct any deviation in the actual value of hypoxia within the chamber, the control unit allows the injection of  $N_2$  into the chamber from a gas source. The setting performance was successfully tested in vivo when subjecting mice to 11%- $O_2$  chronic hypoxia. This device, requiring a low  $N_2$  supply, may facilitate in vivo experimental research of hypoxia-related diseases.

**Keywords:** oxygen sensor; animal research; gas concentration control;  $CO_2$  monitoring; hypoxia model

## 1. Hardware in Context

Respiratory and cardiovascular diseases are nowadays among the most prevalent ones [1,2], and their high morbidity and mortality are expected to increase further because of the worldwide current epidemics of obesity [3,4] and the rise in life expectancy [5,6]. Owing to either poor air oxygenation in the lungs or inadequate blood circulation and distribution, these diseases usually result in chronic hypoxia, a state of poor oxygenation of the cells in tissues and organs. Hypoxia severely affects normal cell function, resulting in negative consequences in multiple organs, such as myocardial ischemia, metabolic diseases, chronic heart and kidney diseases, reproductive diseases, and cancer [7]. Hence, hypoxia plays a relevant pathophysiological role in human health and is a subject of intense investigation [8].

## Specifications table

|                           |   |
|---------------------------|---|
| Hardware name             | Device for subjecting rodents to chronic hypoxia with minimal nitrogen supply                                 |
| Subject area              | Experimental biology and biomedicine  |
| Hardware type             | Device for biomedical animal research   |
| Closest commercial analog | No commercial analog is available   |
| Open source license       | GPL v3  |
| Cost of hardware          | The total cost of the material for the device building is $\approx$ 500 US\$.                                 |
| Source file repository    | <a href="https://data.mendeley.com/datasets/t7dk933sjm/1">https://data.mendeley.com/datasets/t7dk933sjm/1</a> |

Research on the mechanisms involved in the multiorgan consequences of normobaric hypoxia requires animal models based on chronically breathing air with O<sub>2</sub> concentration below the usual 21% of atmospheric air. The most common experimental setting for achieving hypoxia in animal models is to place them into a chamber where the O<sub>2</sub> concentration in the ambient air is reduced by injecting a flow of N<sub>2</sub> [9,10]. Indeed, regulating the flow of room air and of N<sub>2</sub> entering the chamber is the simplest way to control the concentration of O<sub>2</sub> the animals breathe. However, a relatively high flow of N<sub>2</sub> is required since, to prevent hypercapnia, the injected gas must sufficiently wash out the CO<sub>2</sub> exhaled by the animals.

In most cases, the source of N<sub>2</sub> required for the most conventional setting to continuously subject animals to hypoxia cannot be based on conventional bottles of compressed gas because of the high consumption required. A possible option would be an N<sub>2</sub> generator (based on N<sub>2</sub> extraction from room air by a pressure swing adsorption concentrator). However, these devices are expensive, limiting their use for this application. The most common alternative is a centralized N<sub>2</sub> gas pipeline system installed in the building to provide gas to different points of use. However, this infrastructure, which is commonly available in hospitals and cell biology laboratories, is usually unavailable in most animal laboratory facilities. Such requirements for a continuous N<sub>2</sub> source limit the widespread extension of hypoxia-related *in vivo* research.

To facilitate the research employing hypoxic animal models in facilities not having access to a continuous high-flow N<sub>2</sub> source, we aimed to design, build, and test an open-source, low-cost device requiring minimal N<sub>2</sub> provision.

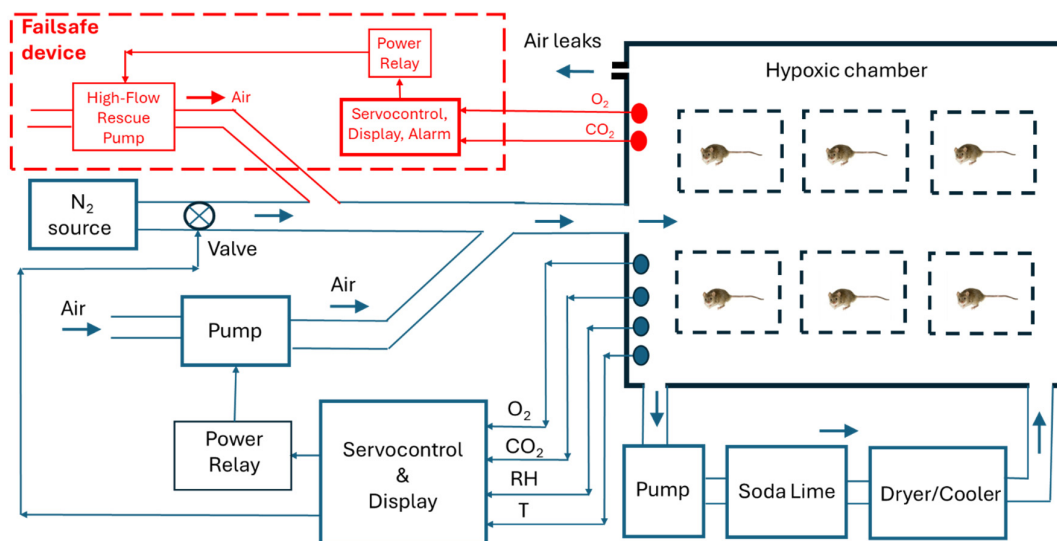
## 2. Hardware Description

### 2.1. Principle of Functioning

Contrary to most conventional settings for producing hypoxic air by continuous N<sub>2</sub> injection, the device described here aims to minimize the supply of N<sub>2</sub> when subjecting mice to controlled chronic hypoxia. The setting is based on ensuring the balance of the gases involved in mice metabolism, thus providing the O<sub>2</sub> consumed and eliminating the exhaled CO<sub>2</sub> and water vapor. A schematic description of the setting is presented in Figure 1: The O<sub>2</sub> and CO<sub>2</sub> concentrations, the relative humidity (RH), and temperature (T) inside the hypoxic chamber are continuously measured by sensors, and processed by the control and display unit, based on an Arduino microcontroller. A high-resistance air leak communicates the hypoxic chamber with the atmospheric air. The air is continuously recirculated within the chamber by the use of a domestic aquarium membrane-based pump (60 l/min). A soda lime filter is used to absorb the generated CO<sub>2</sub>. Medical grade soda lime should be used since it contains ethyl violet, a pH-sensitive dye which changes from colorless to violet as the soda lime absorbs CO<sub>2</sub>. A dryer/cooler (based on an AC 12V 120W liquid-cooling thermoelectric Peltier-based unit providing cool water that circulates through an air radiator) is used to regulate the temperature and to condense water vapor (Figure 1, bottom). For this purpose, the dryer/cooler section is enclosed into a thermally isolating box made with polystyrene walls including an outlet to extract the condensed water (Figure 1, bottom).

A second domestic aquarium pump (30 l/min) is used to introduce room air into the hypoxic chamber to supply the O<sub>2</sub> consumed by the mice. Ideally, the setting would not require any additional N<sub>2</sub> injection to keep a target level of hypoxia since the consumption of O<sub>2</sub> and the production of CO<sub>2</sub> and water vapor are balanced by the components of the setting (Figure 1). However, the control unit allows the injection of N<sub>2</sub> into the chamber from a gas bottle through an electrically controlled valve.

Figure 1 includes (in red) a completely independent (and optional) failsafe device to protect the animals against accidental life-threatening hypoxia or hypercapnia occurred in case any component (e.g., power, pumps, sensors, microprocessors) of the hypoxia device fails. The failsafe device has its own power source, O<sub>2</sub> and CO<sub>2</sub> sensors and Arduino control loop. The gas concentrations are continuously sensed and displayed, and in case concentrations of O<sub>2</sub> is below 8% or CO<sub>2</sub> is above 2000 ppm, both light and sound alarms are activated, and a high-flow (60 l/min) air pump (similar to the ones described for the hypoxic device) is activated to flush room air into the chamber. Using the failsafe device is not strictly required for the normal function of the hypoxic setting but it is strongly recommended. To avoid confusions, the technical description of the independent failsafe device is provided in a specific folder of Supplementary materials.



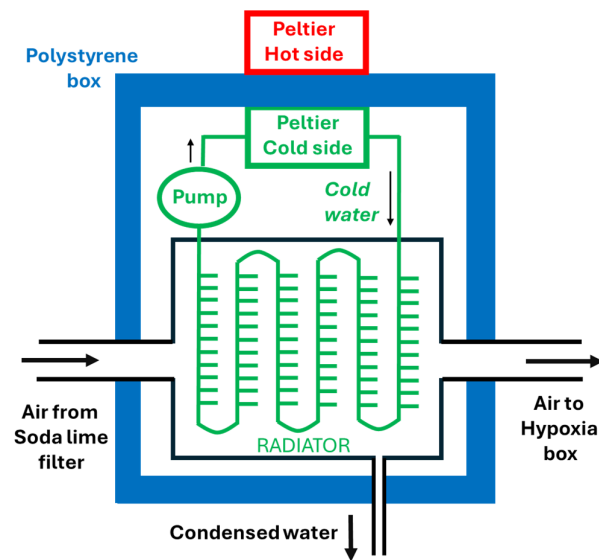


**Figure 1.** Top: Diagram of the hypoxia setting for mice. RH and T are relative humidity and temperature, respectively. O<sub>2</sub> and CO<sub>2</sub> indicate gas concentrations. A completely independent failsafe device is indicated in red. Bottom: Diagram of the Dryer/Cooler. See text for explanation.

The specific device we implemented (Figure 2) was designed to expose up to 30 adult mice to chronic normobaric hypoxia. The hypoxic chamber made with transparent methacrylate walls (4 mm width; dimensions 50 x 61 x 84 cm) allowed to easily accommodate 6 conventional mice cages (17 x 20 x 39 cm) for 5 animals each. The design of the setting was based on the analysis of the physiological variables corresponding to the demanding conditions of 30 mice with the highest possible adult weight of 40 g each, as explained in the following subsections. The dimensions and specifications of the different components can be modified as required if changing the number of mice or the animal species (e.g., rats or guinea pigs).

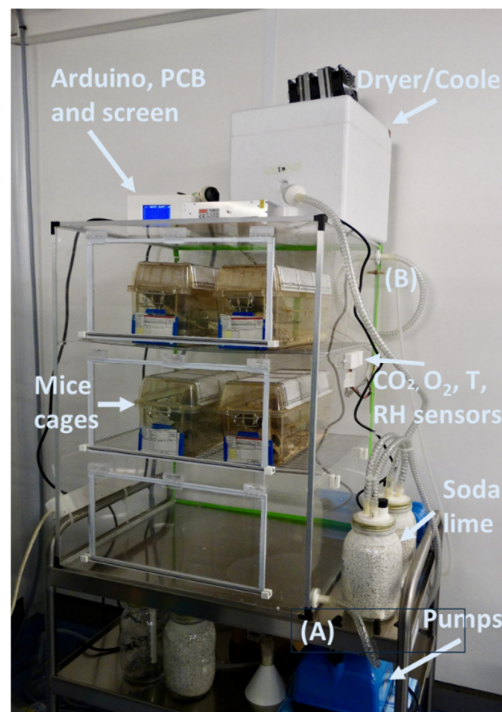


**Figure 2.** Picture of the implemented hypoxic setting with capacity for 30 mice. The chamber air is taken from (A) and, after passing through the soda line and dryer-cooler, is reintroduced into the chamber at a distant point (B) to create a gas circulation that homogenizes gas concentration into the chamber.

## 2.2. Oxygen Balance

The typical rate of  $O_2$  consumption in a mouse is  $0.06 \text{ ml} \cdot (\text{min} \cdot \text{g})^{-1}$  [11]. Therefore, the total oxygen flow consumed ( $V'_{O_2}$ ) by the mice is  $\approx 72 \text{ ml} \cdot \text{min}^{-1}$ . The value of oxygen fraction ( $F_iO_2$ ) in the hypoxic chamber that the user sets on the front panel of the control unit is achieved by mixing the flow of room air ( $V'_{air}$ ) and the  $N_2$  flow ( $V'_{N_2}$ ) entering from the  $N_2$  source. The  $O_2$  flow entering the chamber is the amount introduced by the air pump ( $21\% \cdot V'_{air}$ ). The total flow of  $O_2$  leaving the chamber is the addition of metabolic consumption ( $V'_{O_2}$ ) and the  $O_2$  contained in the total gas leaving the chamber ( $V'_{N_2} + V'_{air}$ ) which is at  $F_iO_2$ . Thus,  $0.21 \cdot V'_{air} = V'_{O_2} + F_iO_2 \cdot (V'_{air} + V'_{N_2})$ , and hence  $V'_{air} = (V'_{O_2} + V'_{N_2} \cdot F_iO_2) / (0.21 - F_iO_2)$ . After an initial injection of  $N_2$  to achieve the desired level of hypoxia, e.g., a target  $F_iO_2 = 0.11$ , minimization of further  $N_2$  consumption ( $V'_{N_2} \approx 0$ ) during steady-state hypoxia would require  $V'_{air} = 720 \text{ ml} \cdot \text{min}^{-1}$  for  $V'_{O_2} = 72 \text{ ml} \cdot \text{min}^{-1}$ . This  $F_iO_2$  value is, in practice, ensured by using the  $O_2$  sensor signal to control the power of the pump injecting the airflow  $V'_{air}$  into the chamber.

## 2.3. $CO_2$ Balance

A critical condition to be achieved inside the hypoxic chamber is normocapnia since the setting would tend to induce hypercapnia by the potential accumulation of the  $CO_2$  produced by mice metabolism. Assuming that the ratio between  $CO_2$  production and  $O_2$  consumption, commonly known as respiratory exchange rate (RER), is equal to 1 in mice [11], the total flow of  $CO_2$  metabolically produced ( $V'_{CO_2}$ ) is  $\approx 72 \text{ ml} \cdot \text{min}^{-1}$ . In case the  $CO_2$  fraction in the chamber ( $F_iCO_2$ ) was simply the result of the washout induced by the total circulating air ( $V'_{air} + V'_{N_2}$ ), i.e., no  $CO_2$  absorption by soda lime, the  $CO_2$  entering the chamber by mice metabolism would be balanced by the  $CO_2$  leaving the chamber. Under a steady state with minimal  $N_2$  supply ( $V'_{N_2} \approx 0$ ,  $V'_{air} = 720 \text{ ml} \cdot \text{min}^{-1}$ ),  $CO_2$  washout would be negligible. Accordingly, the only effective way to reduce  $CO_2$  accumulation in the chamber is by continuously pumping a flow ( $V'_{sl}$ ) of the chamber air through a soda lime canister acting as a  $CO_2$  absorber. Then, the  $CO_2$  metabolically produced ( $V'_{CO_2} = 72 \text{ ml} \cdot \text{min}^{-1}$ ) is balanced by the  $CO_2$  absorbed by the soda lime ( $V'_{sl} \cdot F_iCO_2$ ) and the negligible amount of  $CO_2$  leaving the chamber ( $V'_{air} \cdot F_iCO_2$ ). Hence, for a pump flow  $V'_{sl} = 60 \text{ l} \cdot \text{min}^{-1}$ , the increase in  $F_iCO_2$  would be of only  $\approx 72 \text{ ml} \cdot \text{min}^{-1} / 60000 \text{ ml} \cdot \text{min}^{-1} = 12 \cdot 10^{-4}$  or 1200 ppm (0.12%) above the typical  $F_iCO_2$  of room air, hence a safe value [12]. Since 1 kg of soda lime can absorb up to 260 l of  $CO_2$  [13], the soda lime required to drain the  $72 \text{ ml} \cdot \text{min}^{-1}$  of  $CO_2$  production is 520 g·day<sup>-1</sup>.

## 2.4. Water Vapor Balance

Typical ventilation in mice is  $1.46 \text{ ml} \cdot \text{g}^{-1}$  [14], thus the total respiratory minute volume ( $V'_{min}$ ) is  $\approx 1752 \text{ ml} \cdot \text{min}^{-1}$ . Water vapor is released by mice metabolism, mainly through breathing, thus tending to increase the relative humidity ( $RH$ ) in the chamber air. Expiratory air (at  $37^\circ\text{C}$  and water vapor saturated) and inspiratory air (at chamber temperature and  $RH_b$ ) contain different amounts of water vapor. Taking into account that the partial pressure of water vapor ( $P_{H2O,sat}$ ) at  $37^\circ\text{C}$  is 47 mmHg, for  $V'_{min} = 1752 \text{ ml} \cdot \text{min}^{-1}$ , the water vapor content in the exhaled air is  $1752 \text{ ml} \cdot \text{min}^{-1} \cdot (47 / 760) = 108.3 \text{ ml} \cdot \text{min}^{-1}$ . As  $P_{H2O,sat}(25^\circ\text{C}) = 23.8 \text{ mmHg}$ , the water vapor in the inhaled air content is  $1752 \text{ ml} \cdot \text{min}^{-1} \cdot (23.8 / 760) \cdot RH_b = 54.9 \cdot RH_b \text{ ml} \cdot \text{min}^{-1}$ . Hence, the net water vapor produced by breathing is the difference content in expired and inspired air ( $108.3 - 54.9 \cdot RH_b$ )  $\text{ml} \cdot \text{min}^{-1}$ . Thus, to keep  $RH_b$  at a reasonable value of 60%, a common value in lab animal facilities, the water vapor flow to be eliminated is 75.4 ml/min. Adding the water vapor released by mice transepithelial evaporation (which amounts to  $\approx 50\%$  of water vapor loss by breathing [15],  $\approx 113 \text{ ml/min}$  of water vapor should be eliminated by the air dryer to avoid excessive humidification of the hypoxic chamber air. This amount of water vapor is eliminated by condensation in the cool dryer, specifically by cooling the

airflow ( $V'_{sl} = 60000$  l/min) that is already circulated through soda lime to maintain normocapnia. Indeed, if a flow ( $V'_{sl}$ ) of chamber air ( $RH_b = 60\%$ ,  $25^\circ\text{C}$ , thus containing  $1128$  ml/min of water vapor) is circulated through a refrigerated element that cools the air to a temperature ( $T_c$ ), the maximum content of water vapor in the refrigerated air will be reduced and thus the exceeding amount will condensate on the inner walls of the cooler. The maximum flow of water vapor contained by saturated cooled airflow  $V'_{sl}$  at  $T_c$  is  $60000 \text{ ml/min} \cdot P_{H2O,sat}(T_c) / 760 = 79 \text{ ml/min} \cdot P_{H2O,sat}(T_c)$ . Hence, the liquid water condensed by cooling  $V'_{sl}$  from  $25^\circ\text{C}$  to  $T_c$  is  $1128 - 79 \cdot P_{H2O,sat}(T_c)$ . Accordingly, to eliminate the  $\approx 113$  ml/min of metabolically-produced water vapor, it is required that  $P_{H2O,sat}(T_c) = 12.8$  mmHg, corresponding to  $T_c \approx 15^\circ\text{C}$ . Hence, a relatively mild  $\approx 10^\circ\text{C}$  refrigeration from  $25^\circ\text{C}$  would be enough.

### 2.5. Head Transfer Balance

The metabolic heat dissipation by 25-g mice at common ambient temperature ( $20\text{--}25^\circ\text{C}$ ) is  $0.5$  Kcal/h [11], and thus the heat dissipated by the 30 mice (40 g each) would be ( $Q'_{met}$ ) is  $\approx 30$  W. The net heat balance in the hypoxic chamber is determined by the positive 30 W metabolically dissipated by the mice, the heat dissipated by the soda lime in the absorption process of  $\text{CO}_2$  (13.7 kcal/mol $\text{CO}_2$ ) [13], which in the setting amounts 2.8 W (for  $\text{CO}_2$  density  $1.8 \text{ g}\cdot\text{l}^{-1}$  at  $20^\circ\text{C}$ ), and the negative heat transfer required for heating the previously cooled airflow  $V'_{sl}$  entering the chamber from  $15^\circ\text{C}$  to  $25^\circ\text{C}$ , which amounts  $-12.0$  W (as computed for air density  $1.2 \text{ g}\cdot\text{l}^{-1}$  and specific heat capacity  $1 \text{ J}\cdot\text{g}^{-1}\cdot\text{K}^{-1}$ ). Hence, the net heat balance is  $\approx 21$  W. Taking into account that the chamber ( $50 \times 61 \times 84 \text{ cm}$ ) has a surface ( $A$ ) of  $2.47 \text{ m}^2$ , that the chamber walls are made of 4-mm width ( $d$ ) transparent polymethyl methacrylate (thermal conductivity:  $K = 0.18 \text{ W}\cdot\text{m}^{-1}\cdot\text{K}^{-1}$ ), and that the basic equation for heat transfer is  $Q' = K \cdot A \cdot \Delta T \cdot d^{-1}$ , it results that passive dissipation of  $Q' = 21$  W through the chamber walls would be achieved for a  $\Delta T \leq 0.2^\circ\text{C}$ . Hence, heat transfer balance is achieved for a hypoxic chamber temperature that minimally differs from room temperature.

## 3. Design Files Summary

All the design and software files necessary to build the device presented in this work are distributed under the GPL v3 license and they can be found in the supplementary materials of this manuscript at the following public repositories (DOI: 10.17632/t7dk933sjm.1)

<https://data.mendeley.com/datasets/t7dk933sjm/1>

**Table 1.** Files summary.

| Design file name    | File type        | Open source license | Location of the file |
|---------------------|------------------|---------------------|----------------------|
| Enclosures and lids | STL              | GPL v3              | STL files folder     |
| Code                | ino file         | GPL v3              | Arduino Code folder  |
| PCB Layout          | pdf and jpg file | GPL v3              | Electronics folder   |

## 4. Bill of Materials Summary

The total cost of the materials for building the device is 633,77€. Materials such as resistors, LEDs, pin connectors, capacitors, PCB, ICs, and fuse holders were purchased as a kit, however, not all materials available in the set were used when building a single device. Most of them can be also easily reused from obsolete/damaged consumer electronic devices or household appliances.

| Component                                     | Quantity | Cost per unit € | Total cost € | Source of materials   |
|---|----------|-----------------|--------------|---|
| Sensor O2                                     | 1        | 62,30           | 62,30        | <a href="https://es.farnell.com/dfrobot/sen0322/i2c-oxygen-sensor-module-arduino/dp/3879708?gad_source=1&amp;CMP=KNC-GES-GEN-SHOPPING-Pmax-Catch-all-05-Dec-23&amp;gross_price=true">https://es.farnell.com/dfrobot/sen0322/i2c-oxygen-sensor-module-arduino/dp/3879708?gad_source=1&amp;CMP=KNC-GES-GEN-SHOPPING-Pmax-Catch-all-05-Dec-23&amp;gross_price=true</a>   |
| Sensor CO2, temperature and relative humidity | 1        | 61,14           | 61,14        | <a href="https://es.farnell.com/seeed-studio/101020952/m-dulo-sensor-arduino-raspberry/dp/4007751?st=modulo%20sensor%20%20co2">https://es.farnell.com/seeed-studio/101020952/m-dulo-sensor-arduino-raspberry/dp/4007751?st=modulo%20sensor%20%20co2</a>   |
| Voltage regulator 5V                          | 2        | 0,286           | 0,56         | <a href="https://www.amazon.com/valores-Paquete-regulador-positivo-corriente/dp/B07T5ZHY63/ref=sr_1_1_sspa?__mk_es_US=%C3%85M%C3%85%C5%BD%C3%95%C3%91&amp;crid=1651XJCJY90X&amp;dib=eyJ2IjoiMSJ9.z7VZ01yDMzS7FNoFVZYjIIIDiqJf7MWuKacqC0FVcexkbaaq2K3koWWNRLSjCUnNocgOZhSxSL_K2NLBBZrMZcpmaEX61JZhaHNEK6GLgpEYKA2nXRwSKnqndWUS3hKDUTBenbCbF9ouzxqIJhS3vUE_hhOFrJp8Tlc9ngNTITlqc6fLt1BAs_ijswPUxupFI1jSGK1IUobc-yQ_mRvK1zIJFYo4byvBh0iwoiQtwk.e5isTzn0mwmTiPh46biH3ZfvGoMPDzyBZDeiYAUNsKQ&amp;dib_tag=se&amp;keywords=voltage+regulator+7809&amp;qid=1749637707&amp;sprefix=voltage+regulator+7809%2Caps%2C158&amp;sr=8-1-spons&amp;sp_csd=d2lkZ2V0TmFtZT1zcF9hdGY&amp;psc=1">https://www.amazon.com/valores-Paquete-regulador-positivo-corriente/dp/B07T5ZHY63/ref=sr_1_1_sspa?__mk_es_US=%C3%85M%C3%85%C5%BD%C3%95%C3%91&amp;crid=1651XJCJY90X&amp;dib=eyJ2IjoiMSJ9.z7VZ01yDMzS7FNoFVZYjIIIDiqJf7MWuKacqC0FVcexkbaaq2K3koWWNRLSjCUnNocgOZhSxSL_K2NLBBZrMZcpmaEX61JZhaHNEK6GLgpEYKA2nXRwSKnqndWUS3hKDUTBenbCbF9ouzxqIJhS3vUE_hhOFrJp8Tlc9ngNTITlqc6fLt1BAs_ijswPUxupFI1jSGK1IUobc-yQ_mRvK1zIJFYo4byvBh0iwoiQtwk.e5isTzn0mwmTiPh46biH3ZfvGoMPDzyBZDeiYAUNsKQ&amp;dib_tag=se&amp;keywords=voltage+regulator+7809&amp;qid=1749637707&amp;sprefix=voltage+regulator+7809%2Caps%2C158&amp;sr=8-1-spons&amp;sp_csd=d2lkZ2V0TmFtZT1zcF9hdGY&amp;psc=1</a> |

|                   |   |           |     |   |
|-------------------|---|-----------|-----|---|
| and<br>9V         |   |           |     |   |
| Diode             | 1 | 0,04<br>4 | 0,0 | <a href="https://www.amazon.com/conmutaci%C3%B3n-miliamp-voltios-silicio-electr%C3%B3nicos/dp/B07Q4F3Y5W/ref=sr_1_1_sspa?crid=19S08TO69SSPJ&amp;dib=eyJ2IjoiMSJ9.G4ZHuurkn3IVHsyuKzuoxxIKGXN42qvZAc9mcrW5r69d231gJdkC9262W6Y9Ge7VLNqRy653RUZFWEvndlAY5xd59nQGcFeStJKJ1_vYzKzwS6160cq9R0J4r7gITSLqXn6BMuL67mi8kVQTMqTT2NHGUpl0ptQOIsJUrpLD2EnGLzXHuZAQ9FXGqVdy_-a-TAHyH_NyhFEjnBrFpiu8voqXx_8EnP7By8SCqog0cLuR0ymxSKV6cAbdcwyaRp9ebK8oHe41a7807tuTpKDn0sVd7oFUAog0Dy4GwfcQmjw.AWgWGJvW0Wjxyzk9oo0Ga_ChksybQGJP_y22Lfu2cvI&amp;dib_tag=se&amp;keywords=in4148&amp;qid=1749637823&amp;sprefix=%2Caps%2C115&amp;sr=8-1-spons&amp;sp_csd=d2lkZ2V0TmFtZT1zcF9hdGY&amp;psc=1">https://www.amazon.com/conmutaci%C3%B3n-miliamp-voltios-silicio-electr%C3%B3nicos/dp/B07Q4F3Y5W/ref=sr_1_1_sspa?crid=19S08TO69SSPJ&amp;dib=eyJ2IjoiMSJ9.G4ZHuurkn3IVHsyuKzuoxxIKGXN42qvZAc9mcrW5r69d231gJdkC9262W6Y9Ge7VLNqRy653RUZFWEvndlAY5xd59nQGcFeStJKJ1_vYzKzwS6160cq9R0J4r7gITSLqXn6BMuL67mi8kVQTMqTT2NHGUpl0ptQOIsJUrpLD2EnGLzXHuZAQ9FXGqVdy_-a-TAHyH_NyhFEjnBrFpiu8voqXx_8EnP7By8SCqog0cLuR0ymxSKV6cAbdcwyaRp9ebK8oHe41a7807tuTpKDn0sVd7oFUAog0Dy4GwfcQmjw.AWgWGJvW0Wjxyzk9oo0Ga_ChksybQGJP_y22Lfu2cvI&amp;dib_tag=se&amp;keywords=in4148&amp;qid=1749637823&amp;sprefix=%2Caps%2C115&amp;sr=8-1-spons&amp;sp_csd=d2lkZ2V0TmFtZT1zcF9hdGY&amp;psc=1</a> |
| Transistor        | 1 | 0,28<br>8 | 0,2 | <a href="https://www.amazon.com/valores-transistor-potencia-epitaxial-Darlington/dp/B08BFYVK6C/ref=sr_1_2_sspa?__mk_es_US=%C3%85M%C3%85%C5%BD%C3%95%C3%91&amp;crid=F7L9BPIUJJ1J&amp;dib=eyJ2IjoiMSJ9.h3cxIy3MyTNjNTX3uCvtQcwfWZK_sKfZ5uAxLmZxsqRtPa0gU6bxTYAyV5DnWuyAXByYs1n1nX0i6Q_l5MTe88pNAxBZxrPfEn8voxaQCTiZdJVnQwGgVRG-ODWzeXTkUsD0i6EbqcQMcgAnbQ2VqfPOWZgFRMchaxT0K9n_Gp6LGWk1V-iedqbZlpo_bcyz1OLHvcxVl1vjiv74yYgciAfzE5yGDDIyRHC4q1iHCw.mcSg2LgzbVTPOuRlbtI4MDXSFdDEva1NHrZGLCBTpZU&amp;dib_tag=se&amp;keywords=tip122&amp;qid=1749637875&amp;sprefix=tip12%2Caps%2C198&amp;sr=8-2-spons&amp;sp_csd=d2lkZ2V0TmFtZT1zcF9hdGY&amp;psc=1">https://www.amazon.com/valores-transistor-potencia-epitaxial-Darlington/dp/B08BFYVK6C/ref=sr_1_2_sspa?__mk_es_US=%C3%85M%C3%85%C5%BD%C3%95%C3%91&amp;crid=F7L9BPIUJJ1J&amp;dib=eyJ2IjoiMSJ9.h3cxIy3MyTNjNTX3uCvtQcwfWZK_sKfZ5uAxLmZxsqRtPa0gU6bxTYAyV5DnWuyAXByYs1n1nX0i6Q_l5MTe88pNAxBZxrPfEn8voxaQCTiZdJVnQwGgVRG-ODWzeXTkUsD0i6EbqcQMcgAnbQ2VqfPOWZgFRMchaxT0K9n_Gp6LGWk1V-iedqbZlpo_bcyz1OLHvcxVl1vjiv74yYgciAfzE5yGDDIyRHC4q1iHCw.mcSg2LgzbVTPOuRlbtI4MDXSFdDEva1NHrZGLCBTpZU&amp;dib_tag=se&amp;keywords=tip122&amp;qid=1749637875&amp;sprefix=tip12%2Caps%2C198&amp;sr=8-2-spons&amp;sp_csd=d2lkZ2V0TmFtZT1zcF9hdGY&amp;psc=1</a>   |
| Solid state Relay | 1 | 2,20<br>0 | 2,2 | <a href="https://www.amazon.com/-/es/HiLetgo-m%C3%B3dulo-estado-Control-fusible/dp/B00WSN9CJC/ref=sr_1_6?__mk_es_US=%C3%85M%C3%85%C5%BD%C3%95%C3%91&amp;crid=1DCI0ST74VCPI&amp;dib=eyJ2IjoiMSJ9.q91PYm6OKAKVxQl4ebBf0AcV_wFfLUw6yFpImY74y9NNuAwuMA_hpIqRP2tM66p4flq29UABM9fa-Vt8GxLx1_6p2ie44_AJ84mtp5V95vCcb2_E7tkDR2bruMwsij8DGnkhkGYR3yGb3K202Yot5Uw3FOzQ5Em4ew4ZXLH8U5mn9tf4yMoJdQZ_yI1NPchNJZzmKsWA_Omo89YqgdAJFDpTr6nQ7RvzFNO0pdqxyZg.B-yP_CUBkbA0UKhlF3XE1GJNXnzZo4iaBUsoYxd5gl0&amp;dib_tag=se&amp;keywords=rele+solid+state+5V&amp;qid=1749637984&amp;sprefix=rele+solid+state+5v%2Caps%2C131&amp;sr=8-6">https://www.amazon.com/-/es/HiLetgo-m%C3%B3dulo-estado-Control-fusible/dp/B00WSN9CJC/ref=sr_1_6?__mk_es_US=%C3%85M%C3%85%C5%BD%C3%95%C3%91&amp;crid=1DCI0ST74VCPI&amp;dib=eyJ2IjoiMSJ9.q91PYm6OKAKVxQl4ebBf0AcV_wFfLUw6yFpImY74y9NNuAwuMA_hpIqRP2tM66p4flq29UABM9fa-Vt8GxLx1_6p2ie44_AJ84mtp5V95vCcb2_E7tkDR2bruMwsij8DGnkhkGYR3yGb3K202Yot5Uw3FOzQ5Em4ew4ZXLH8U5mn9tf4yMoJdQZ_yI1NPchNJZzmKsWA_Omo89YqgdAJFDpTr6nQ7RvzFNO0pdqxyZg.B-yP_CUBkbA0UKhlF3XE1GJNXnzZo4iaBUsoYxd5gl0&amp;dib_tag=se&amp;keywords=rele+solid+state+5V&amp;qid=1749637984&amp;sprefix=rele+solid+state+5v%2Caps%2C131&amp;sr=8-6</a>   |
| Connectors        | 6 | 0,11<br>6 | 0,6 | <a href="https://www.amazon.com/s?k=conectores+arduino&amp;__mk_es_US=%C3%85M%C3%85%C5%BD%C3%95%C3%91&amp;crid=ZOJGKBHPROE&amp;sprefix=conectores+arduino%2Caps%2C133&amp;ref=nb_sb_noss">https://www.amazon.com/s?k=conectores+arduino&amp;__mk_es_US=%C3%85M%C3%85%C5%BD%C3%95%C3%91&amp;crid=ZOJGKBHPROE&amp;sprefix=conectores+arduino%2Caps%2C133&amp;ref=nb_sb_noss</a>   |
| Capacitors        | 4 | 0,04<br>6 | 0,1 | <a href="https://www.amazon.com/ALLECIN-surtido-condensadores-electrol%C3%B3ticos-aluminio/dp/B0C1VBXCQM/ref=sr_1_1_sspa?__mk_es_US=%C3%85M%C3%85%C5%BD%C3%95%C3%91&amp;crid=O5JYUB0HNKY2&amp;dib=eyJ2IjoiMSJ9.ekYH7j2EeGYfnpDMkTUbA5_8nAZM5NXRF7ISTCDYRdiGRRate4MlrQd9ldvZs-A_pzD-zjApyYWkhjoUOqNALpVcJsc6DD3JHlReRoBcxMOy5HnZgoPPDGKGQ7eKiroLYErIckXUuGwYEHo_DbuP4dZ3WHupx5R5NgErb4ax20-">https://www.amazon.com/ALLECIN-surtido-condensadores-electrol%C3%B3ticos-aluminio/dp/B0C1VBXCQM/ref=sr_1_1_sspa?__mk_es_US=%C3%85M%C3%85%C5%BD%C3%95%C3%91&amp;crid=O5JYUB0HNKY2&amp;dib=eyJ2IjoiMSJ9.ekYH7j2EeGYfnpDMkTUbA5_8nAZM5NXRF7ISTCDYRdiGRRate4MlrQd9ldvZs-A_pzD-zjApyYWkhjoUOqNALpVcJsc6DD3JHlReRoBcxMOy5HnZgoPPDGKGQ7eKiroLYErIckXUuGwYEHo_DbuP4dZ3WHupx5R5NgErb4ax20-</a>   |



|   |                             |                   |                |   |
|---|-----------------------------|-------------------|----------------|---|
|   |                             |                   |                | 0bVA56GPbf6AHFW0x2BVjzMCRqJcM72pPARxXIipVztftF2eEvVnVx2oaxKJv7E.rax_WABdj5Kg3iZg0-<br>DCwqXoqhX58FBhrXxgFDcFrk&dib_tag=se&keywords=condensadores&qid=1749638632&sprefix=condensadore%2Caps%2C169&sr=8-1-<br>spons&sp_csd=d2lkZ2V0TmFtZT1zcF9hdGY&psc=1  |
| Ardui<br>no<br>Mega                                       | 1<br>23,2<br>5<br>23,<br>25 | 23,<br>5<br>25    | 23,<br>5<br>25 | <a b0d6b9m4zh="" binghe-bol%c3%adgrafo-contacto-resoluci%c3%b3n-b3n-compatible="" dp="" href="https://www.amazon.es/ELEGOO-Microcontrolador-ATmega2560-ATmega16U2-Compatible/dp/B06Y3ZHPWC/ref=sr_1_2_sspa?__mk_es_ES=%C3%85M%C3%85%C5%BD%C3%95%C3%91&amp;qid=16IXP8IYVEZIP&amp;dib=eyJ2IjoiMSJ9.VNIP3CQ0NzQDPWLu2uC7KkHA_lwuDLf45_9fQSmtbWX2NOfw9qL2kbiUGF2MnDCMVOVg4_-bUWaN20Oo-pyASW_fsBa_0BKxKMCKOIPvQIcAQR6LkANQDjtDT_nyyHx2ukyr-PD484nwxI2IANpNtI_E-62_pEWMiufkU8QHl7q1S8JpvGJMcdeHwqG-1ufXxIfMmGLtVCMEVGeAfOb1MSvMF3AFAV1wK7aIIIRbpWm8kf6G-NnivmR22WzIv0Qw8t_W8qhw9jDU8I6Lsm2-z2Id8eIaxHEbcPxL0E-4.c8KUwVEiJ7T0gRfOboB311pEUyYhsvdQTWCAj5wkmN4&amp;dib_tag=se&amp;keywords=arduino+mega+con+pantalla&amp;qid=1749642004&amp;sprefix=arduino+mega+con+pantalla%2Caps%2C90&amp;sr=8-2-spons&amp;sp_csd=d2lkZ2V0TmFtZT1zcF9hdGY&amp;psc=1&lt;/a&gt;&lt;/td&gt;&lt;/tr&gt; &lt;tr&gt; &lt;td&gt;Scree&lt;br/&gt;n 3,5''&lt;/td&gt;&lt;td&gt;1&lt;br/&gt;18,9&lt;br/&gt;9&lt;br/&gt;99&lt;/td&gt;&lt;td&gt;18,&lt;br/&gt;9&lt;br/&gt;99&lt;/td&gt;&lt;td&gt;18,&lt;br/&gt;9&lt;br/&gt;99&lt;/td&gt;&lt;td&gt;&lt;a href=" https:="" ref='sr_1_4?__mk_es_ES=%C3%85M%C3%85%C5%BD%C3%95%C3%91&amp;qid=16IXP8IYVEZIP&amp;dib=eyJ2IjoiMSJ9.VNIP3CQ0NzQDPWLu2uC7KkHA_lwuDLf45_9fQSmtbWX2NOfw9qL2kbiUGF2MnDCMVOVg4_-bUWaN20Oo-pyASW_fsBa_0BKxKMCKOIPvQIcAQR6LkANQDjtDT_nyyHx2ukyr-PD484nwxI2IANpNtI_E-62_pEWMiufkU8QHl7q1S8JpvGJMcdeHwqG-1ufXxIfMmGLtVCMEVGeAfOb1MSvMF3AFAV1wK7aIIIRbpWm8kf6G-NnivmR22WzIv0Qw8t_W8qhw9jDU8I6Lsm2-z2Id8eIaxHEbcPxL0E-4.c8KUwVEiJ7T0gRfOboB311pEUyYhsvdQTWCAj5wkmN4&amp;dib_tag=se&amp;keywords=arduino+mega+con+pantalla&amp;qid=1749642106&amp;sprefix=arduino+mega+con+pantalla%2Caps%2C90&amp;sr=8-4"' www.amazon.es="">https://www.amazon.es/Binghe-Bol%C3%ADgrafo-Contacto-Resoluci%C3%B3n-B3n-Compatible/dp/B0D6B9M4ZH/ref=sr_1_4?__mk_es_ES=%C3%85M%C3%85%C5%BD%C3%95%C3%91&amp;qid=16IXP8IYVEZIP&amp;dib=eyJ2IjoiMSJ9.VNIP3CQ0NzQDPWLu2uC7KkHA_lwuDLf45_9fQSmtbWX2NOfw9qL2kbiUGF2MnDCMVOVg4_-bUWaN20Oo-pyASW_fsBa_0BKxKMCKOIPvQIcAQR6LkANQDjtDT_nyyHx2ukyr-PD484nwxI2IANpNtI_E-62_pEWMiufkU8QHl7q1S8JpvGJMcdeHwqG-1ufXxIfMmGLtVCMEVGeAfOb1MSvMF3AFAV1wK7aIIIRbpWm8kf6G-NnivmR22WzIv0Qw8t_W8qhw9jDU8I6Lsm2-z2Id8eIaxHEbcPxL0E-4.c8KUwVEiJ7T0gRfOboB311pEUyYhsvdQTWCAj5wkmN4&amp;dib_tag=se&amp;keywords=arduino+mega+con+pantalla&amp;qid=1749642106&amp;sprefix=arduino+mega+con+pantalla%2Caps%2C90&amp;sr=8-4</a> |
| Cham<br>ber<br>poly<br>meth<br>yl<br>meth<br>acryla<br>te | 2,5<br>m2<br>2(m<br>2)      | 65,7<br>2(m<br>2) | 164<br>,30     | <a href="https://planchasdeplastico.es/producto/polycarbonato-transparente-3-mm/?gad_source=1&amp;gad_campaignid=16996510449&amp;gbraid=0AAAAAAoVwwA-2JSUGanHN_CR0-AZc1Ivjj&amp;gclid=Cj0KCQjw0qTCBhCmARIsAAj8C4Y5dcppkkNshgAS0GoqjeuNiEiCO95D5VttoEFx4nHkqewEDAKf7SoaAnJJEALw_wcB">https://planchasdeplastico.es/producto/polycarbonato-transparente-3-mm/?gad_source=1&amp;gad_campaignid=16996510449&amp;gbraid=0AAAAAAoVwwA-2JSUGanHN_CR0-AZc1Ivjj&amp;gclid=Cj0KCQjw0qTCBhCmARIsAAj8C4Y5dcppkkNshgAS0GoqjeuNiEiCO95D5VttoEFx4nHkqewEDAKf7SoaAnJJEALw_wcB</a>   |
| Rack  | 3<br>0                      | 11,0<br>00        | 33,<br>00      | <a href="https://www.amazon.es/Mallard-Ferri%C3%A8re-cromado-rejilla-60/dp/B00BMKWP5U/ref=sr_1_7?__mk_es_ES=%C3%85M%C3%85%C5%BD%C3%95%C3%91&amp;qid=2V6WL13VKL0ZY&amp;dib=eyJ2IjoiMSJ9.D1aLnzF4G36EJHCIT1wbHuzBq6CHue7ZO_5WTr09IPf_FcX3ORDatQU4OY5709laVOA0idmW5NpqLC6RQz7T87oYfxrDxjSR5eTrB0yLd1bjZbrDPnmBd7xqRa9mAxg3pcdKftQlQGtVIfaI4jVlV9tNLabpyse-">https://www.amazon.es/Mallard-Ferri%C3%A8re-cromado-rejilla-60/dp/B00BMKWP5U/ref=sr_1_7?__mk_es_ES=%C3%85M%C3%85%C5%BD%C3%95%C3%91&amp;qid=2V6WL13VKL0ZY&amp;dib=eyJ2IjoiMSJ9.D1aLnzF4G36EJHCIT1wbHuzBq6CHue7ZO_5WTr09IPf_FcX3ORDatQU4OY5709laVOA0idmW5NpqLC6RQz7T87oYfxrDxjSR5eTrB0yLd1bjZbrDPnmBd7xqRa9mAxg3pcdKftQlQGtVIfaI4jVlV9tNLabpyse-</a>   |



|                       |   |         |          |   |
|-----------------------|---|---------|----------|---|
|                       |   |         |          | 1ln13VbL5By94Qt2BkDkJo4coagITwtE3pNG-Drcpuch8YyzA4YgWY2huacB4vj4O4oZJ7au3IjG-Y1rjsIMG4AVEJtxHMyniUypJ0bWs_USfhGiPeVA_JXeFG7aufLo6DtSsklo-c.9nLvIyT4-DDJM9Y6EGfGY1Slq_SyAkWfgoQLRpgNxXE&dib_tag=se&keywords=rejilla+60x50&qid=1749639549&sprefix=rejilla+60x50%2Caps%2C83&sr=8-7   |
| Pump 30l/m in         | 1 | 61,1 8  | 61, 18   | <a href="https://www.amazon.es/Hailea-bomba-minuto-incluye-hidrop%C3%B3nico/dp/B00NSOQZO0/ref=sr_1_6?__mk_es_ES=%C3%85M%C3%85%C5%BD%C3%95%C3%91&amp;qid=2QV3ZCZZQW2EP&amp;dib=eyJ2IjoiMSJ9.8EvrXsj1Rve6ppqRPADz0-VaZ0Vpe3Ad9jM2Y01LJHfGVrsnI4xbu3vmb0839HdqjEGE8U7JU9FCOhZENWH55rtt5RVu7eWzqa-n7OEE70Ot9CG2JJupy_W4fQCEEgj1ojhxiMCggONskinhanDqchDC4PTigzll2OZqpo_y1HUKPAySq8f8n4WtXCsYTqWiHs4TX7fCgu7U6xTNvHZS8mB-U7dgI-JvHv9Z9ODIOE6h5fac7dldxlGhVDIBLOF2mTGdx8rXOzodLoEyiE1r_xtG-xHwmzzBBrQsUgGERrc.QgNQ_J8WkHaYqVuGzuyWAp5TwTee0tubDkAzO8SgjEs&amp;dib_tag=se&amp;keywords=bomba+60l%2Fmin&amp;qid=1749639830&amp;sprefix=bomba+60l%2Fmin%2Caps%2C94&amp;sr=8-6">https://www.amazon.es/Hailea-bomba-minuto-incluye-hidrop%C3%B3nico/dp/B00NSOQZO0/ref=sr_1_6?__mk_es_ES=%C3%85M%C3%85%C5%BD%C3%95%C3%91&amp;qid=2QV3ZCZZQW2EP&amp;dib=eyJ2IjoiMSJ9.8EvrXsj1Rve6ppqRPADz0-VaZ0Vpe3Ad9jM2Y01LJHfGVrsnI4xbu3vmb0839HdqjEGE8U7JU9FCOhZENWH55rtt5RVu7eWzqa-n7OEE70Ot9CG2JJupy_W4fQCEEgj1ojhxiMCggONskinhanDqchDC4PTigzll2OZqpo_y1HUKPAySq8f8n4WtXCsYTqWiHs4TX7fCgu7U6xTNvHZS8mB-U7dgI-JvHv9Z9ODIOE6h5fac7dldxlGhVDIBLOF2mTGdx8rXOzodLoEyiE1r_xtG-xHwmzzBBrQsUgGERrc.QgNQ_J8WkHaYqVuGzuyWAp5TwTee0tubDkAzO8SgjEs&amp;dib_tag=se&amp;keywords=bomba+60l%2Fmin&amp;qid=1749639830&amp;sprefix=bomba+60l%2Fmin%2Caps%2C94&amp;sr=8-6</a>   |
| Pump 60l/m in         | 1 | 110, 00 | 110, ,00 | <a href="https://www.amazon.es/AquaForte-aluminio-Silenciosa-Capacidad-regulable/dp/B006SYHCl0/ref=sr_1_5?__mk_es_ES=%C3%85M%C3%85%C5%BD%C3%95%C3%91&amp;qid=1Z9OHLAOKFU5L&amp;dib=eyJ2IjoiMSJ9.NRkweEtIZU8--IlxdeJnBVnA57aO3bZv5hAEsbZEYcl9xBXcXFNMVAeKlU_86n4GJzWpJ4OIB5EVtu1BudyX06OpzDGO0m-QAcaWxxlnw97C1ZDvWj0Q6BCLHxdqOjyrizC-5bgqUftjGLc7AgJx9N7xc5UT6tWYHqjTycqoAMjZkBHAgosIT_-LUFZe5Z_CAMOPIR3IbjEVCJU9N_bvvnFdB68xiLwvSfY2hTURhiUBE75D232bex3DA3G01LUZhVONH23IfRAz2U_0am5jKcT0EFB2WKabKOpAJOVNUM.SmnSqG7K3XQG0_bTTbTVbFH7hzXOCEkY8uRXlZar1lc&amp;dib_tag=se&amp;keywords=Bomba%2Bv30&amp;qid=1749640500&amp;sprefix=bomba%2Bv30%2Caps%2C130&amp;sr=8-5&amp;th=1">https://www.amazon.es/AquaForte-aluminio-Silenciosa-Capacidad-regulable/dp/B006SYHCl0/ref=sr_1_5?__mk_es_ES=%C3%85M%C3%85%C5%BD%C3%95%C3%91&amp;qid=1Z9OHLAOKFU5L&amp;dib=eyJ2IjoiMSJ9.NRkweEtIZU8--IlxdeJnBVnA57aO3bZv5hAEsbZEYcl9xBXcXFNMVAeKlU_86n4GJzWpJ4OIB5EVtu1BudyX06OpzDGO0m-QAcaWxxlnw97C1ZDvWj0Q6BCLHxdqOjyrizC-5bgqUftjGLc7AgJx9N7xc5UT6tWYHqjTycqoAMjZkBHAgosIT_-LUFZe5Z_CAMOPIR3IbjEVCJU9N_bvvnFdB68xiLwvSfY2hTURhiUBE75D232bex3DA3G01LUZhVONH23IfRAz2U_0am5jKcT0EFB2WKabKOpAJOVNUM.SmnSqG7K3XQG0_bTTbTVbFH7hzXOCEkY8uRXlZar1lc&amp;dib_tag=se&amp;keywords=Bomba%2Bv30&amp;qid=1749640500&amp;sprefix=bomba%2Bv30%2Caps%2C130&amp;sr=8-5&amp;th=1</a>   |
| 3D printing           | - | 31,0 0  | 31, 00   | <a href="https://es.farnell.com/ultimaker/1609/filament-pla-black-750g/dp/2992628?gross_price=true&amp;CMP=KNC-GES-GEN-SHOPPING-Pmax-High_ROAS&amp;gad_source=1&amp;gad_campaignid=18071281895&amp;gbraid=0AAAAAD8yeHlKxiGMy79WCfjwNBT_BsqP9&amp;gclid=Cj0KCQjw0qTCBhCmARIsAAj8C4b-IsF7T5oIuiyewkZV-nNr8tDFVX0VY5St76HWuHN5j-02Z0rQICEaAhJBEALw_wcB">https://es.farnell.com/ultimaker/1609/filament-pla-black-750g/dp/2992628?gross_price=true&amp;CMP=KNC-GES-GEN-SHOPPING-Pmax-High_ROAS&amp;gad_source=1&amp;gad_campaignid=18071281895&amp;gbraid=0AAAAAD8yeHlKxiGMy79WCfjwNBT_BsqP9&amp;gclid=Cj0KCQjw0qTCBhCmARIsAAj8C4b-IsF7T5oIuiyewkZV-nNr8tDFVX0VY5St76HWuHN5j-02Z0rQICEaAhJBEALw_wcB</a>   |
| Thermoelectric cooler | 1 | 47,4 1  | 47, 41   | <a href="https://www.amazon.es/Refrigerador-Refrigeraci%C3%B3n-Termoel%C3%A9ctrico-Enfriamiento-Semiconductores/dp/B0F6NWNWJM/ref=sr_1_16?__mk_es_ES=%C3%85M%C3%85%C5%BD%C3%95%C3%91&amp;qid=1XPI9W7G6FJMY&amp;dib=eyJ2IjoiMSJ9.9tY2M3EO0bKYlIISgJaOjbFR0CO1MNnuPKF7FQmBmf24793Shg3oHhO-N_JNhPTuMwtWic163ggGxBsgEaRs6K16S-PeHerDs4niKZfdYLnl9DrVWBIBR1iV60ukXPu3hhjJTvsIpVfQ1XD-gxILKkw2GAAQosMOAUKuB3SloCD-4lxuFh2BLEdseAl5S91JsiijAaGn6LtfQBiloiHr3EaD2cnSsgdszxBCcni6g-tGIKIw5CnGXptQwrq8BEX4UCFTLGcdRjignZ0kLzgelIU7xlUn5pjFYNRXYykJEW0.kDaw92Wqmkk6qb-3Jdq5KTzDpfY6PgVISbfYPW0V8aU&amp;dib_tag=se&amp;keywords=peltier+12v+120W+liquido&amp;qid=1749724430&amp;sprefix=peltier+12v+120w+liquido%2Caps%2C89&amp;sr=8-16">https://www.amazon.es/Refrigerador-Refrigeraci%C3%B3n-Termoel%C3%A9ctrico-Enfriamiento-Semiconductores/dp/B0F6NWNWJM/ref=sr_1_16?__mk_es_ES=%C3%85M%C3%85%C5%BD%C3%95%C3%91&amp;qid=1XPI9W7G6FJMY&amp;dib=eyJ2IjoiMSJ9.9tY2M3EO0bKYlIISgJaOjbFR0CO1MNnuPKF7FQmBmf24793Shg3oHhO-N_JNhPTuMwtWic163ggGxBsgEaRs6K16S-PeHerDs4niKZfdYLnl9DrVWBIBR1iV60ukXPu3hhjJTvsIpVfQ1XD-gxILKkw2GAAQosMOAUKuB3SloCD-4lxuFh2BLEdseAl5S91JsiijAaGn6LtfQBiloiHr3EaD2cnSsgdszxBCcni6g-tGIKIw5CnGXptQwrq8BEX4UCFTLGcdRjignZ0kLzgelIU7xlUn5pjFYNRXYykJEW0.kDaw92Wqmkk6qb-3Jdq5KTzDpfY6PgVISbfYPW0V8aU&amp;dib_tag=se&amp;keywords=peltier+12v+120W+liquido&amp;qid=1749724430&amp;sprefix=peltier+12v+120w+liquido%2Caps%2C89&amp;sr=8-16</a> |
| Water cooling         | 1 | 15,9 9  | 15, 99   | <a href="https://www.amazon.es/CENPEK-Radiador-refrigeraci%C3%B3n-B3n-Intercambiador-computadora/dp/B09FXL787S/ref=sr_1_12?__mk_es_ES=%C3%85M%C3%85%C5%BD%C3%95%C3%91&amp;qid=PQGXMX2YHEEV3&amp;dib=eyJ2IjoiMSJ9.yjbkS_YR53lsFDVB9rz0eYd5sZpphUjuTHx0GHaUkYI5UlNnAXcYGrK5NPn7pJfDK7bzqOrTpZhn_NPlxIlyE2goUsz_bcNBKzDvYGkalZlo9KPsHoiczEU67CN8_tpfdQOO35OF_DK9ZAaofcYhHLr3qrTsUEJqPhkwz7V0">https://www.amazon.es/CENPEK-Radiador-refrigeraci%C3%B3n-B3n-Intercambiador-computadora/dp/B09FXL787S/ref=sr_1_12?__mk_es_ES=%C3%85M%C3%85%C5%BD%C3%95%C3%91&amp;qid=PQGXMX2YHEEV3&amp;dib=eyJ2IjoiMSJ9.yjbkS_YR53lsFDVB9rz0eYd5sZpphUjuTHx0GHaUkYI5UlNnAXcYGrK5NPn7pJfDK7bzqOrTpZhn_NPlxIlyE2goUsz_bcNBKzDvYGkalZlo9KPsHoiczEU67CN8_tpfdQOO35OF_DK9ZAaofcYhHLr3qrTsUEJqPhkwz7V0</a>   |



|                    |   |      |      |  |
|--------------------|---|------|------|--|
| radiat or          |   |      |      | Bg8SO2REwV15OTBLg_uwcM5tloSxGjuGmAhrcS_X7Qrxw18W9LjGTun564uKLiel05dAQiT5TZ6nAGbaw8igOMGZmzpsWvEZrDNOExwrxasGjp5itvNiLNFSgtgyNaFOJc.G1-K8oQzQAXi-uTpVrxW7Fyd0eNC0x3PsQHYMwMlq-4&dib_tag=se&keywords=radiador+liquido&qid=1749724514&sprefix=radiador+liquido%2Caps%2C77&sr=8-12   |
| Water cooling pump | 1 | 19,7 | 19,2 | 72 https://www.amazon.es/Diyeeni-refrigeraci%C3%B3n-expansi%C3%B3n-m%C3%A1x-Bomba-enfriamiento/dp/B07ZRQRV7J/ref=sr_1_4?__mk_es_ES=%C3%85M%C3%85%C5%BD%C3%95%C3%91&qid=2PGY6ZH64SWIS&dib=eyJ2ljoiMSJ9.fLA9IrZ-4xlijiCZDNLlo0iOr0srTdzEtk26K6yuy7gC27QZgzKO3yCZpTJPTes98E8sfvWLDY58QdMIxf7WFjln4dTfSQemugONaQwo8cqYc70UEWTb35qg50KeciM-G5VzBf4mZiaAk483FHoIRd8rsp9fGP9PY_fHRqzVkJfzffeJJaPv2YuOewTKz0QHwzmhtHavNzgWzUONq1C4nojCNiIV_by89kzD9YEq5_OL82FUaG-W6l5QxrdNt7rga4DEEUKZW26d28iO6IUbgxF22iBQ_jiEh9h6o.T2DoqO2ThfgHihFKC9f4l2e8n3kWIol2-tvC-n82Zew&dib_tag=se&keywords=bomba+liquido+refrigeracion&qid=1749724631&sprefix=bomba+liquido+refrigeracion%2Caps%2C77&sr=8-4 |

## 5. Build Instructions

### 5.1. 3D Design and Printing

The chamber was built using polymethylmethacrylate sheets, forming a sealed enclosure with three hinged doors that allow the insertion of mice cages. To ensure proper closure, a metal rod is used to apply pressure on each door against the chamber frame. Custom 3D-printed holders were designed and fabricated to hold the metal rods securely in place. On the side of the chamber, additional 3D-printed holders are used as storage for the metal rods when they are not in use.

Beyond structural mounting, 3D printing was also leveraged to develop custom protective enclosures for the gas sensors affixed to the chamber. These cases were specifically designed with dedicated slots and openings for efficient gas exchange. A custom 3D-printed case was also created to house the electronic circuit incorporating the Arduino board. This enclosure includes ventilation slots to prevent overheating, a front opening for the display module that visualizes real-time data and system graphics, and a rear connector interface for power supply integration. 3D printing was also employed to create accessory components for the soda lime containers. These components ensure optimal airflow for efficient CO<sub>2</sub> removal. Furthermore, a funnel specifically designed for refilling the soda lime containers was also produced using a 3D printer. Figure 3 shows the 3D-printed components.

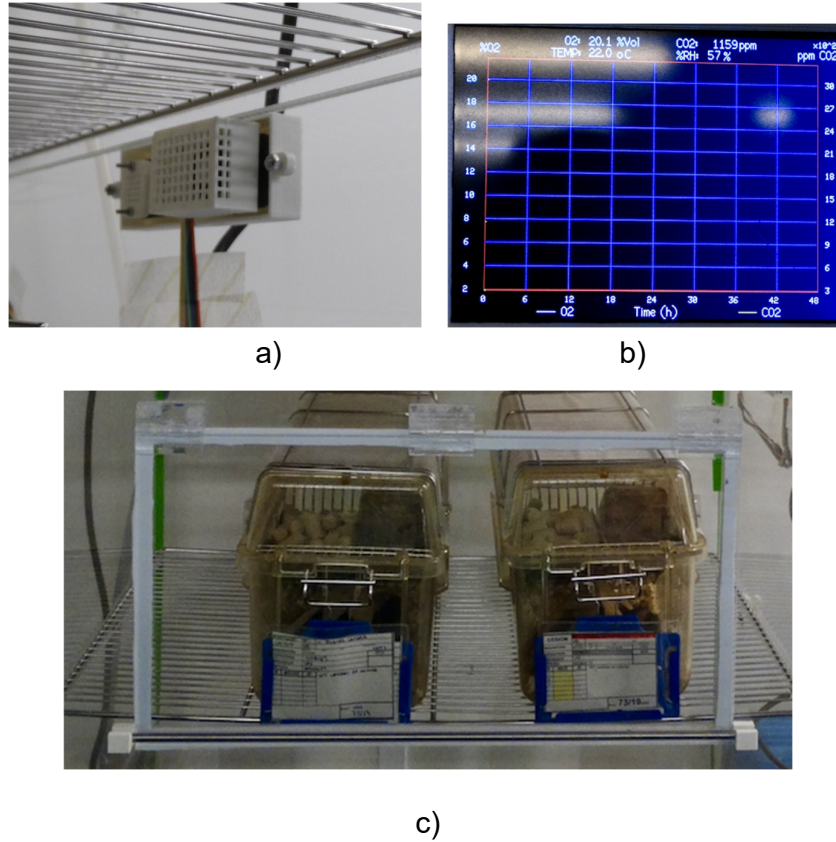


**Figure 3.** 3D-printed components, including the sensor enclosures (a), the Arduino and electronics housing (b), and the metal rod supports used for sealing the chamber doors (c).

### 5.2. Electronics

The electronic system, shown in Figure 4, has been designed to interface the gas sensors with a microcontroller unit (MCU), specifically an Arduino Mega, while also enabling control of electromechanical actuators such as a solenoid valve and pumps via a transistor switch and a solid-state relay, respectively. An I<sup>2</sup>C-based Sensirion SCD4x sensor is employed for measuring CO<sub>2</sub>

concentration, temperature, and humidity, while oxygen levels are monitored using a DFRobot I<sup>2</sup>C oxygen sensor module. The schematic is organized into distinct functional blocks: sensor interfacing, power regulation, and actuator control. The system operates from a single 12V DC power source. Two linear voltage (7805 for 5V and 7809 for 9V) regulators are used to derive the required supply voltages for the other components.

The injection of N<sub>2</sub> into the chamber is allowed by a solenoid valve driven by TIP122 NPN Darlington transistor that acts as a switch. A flyback diode (1N4148) is placed in parallel with the solenoid coil to protect the transistor from voltage spikes. This valve remains closed except when activated. The introduction of room air through the pump is controlled via a digitally-activated solid-state relay, which provides electrical isolation and long-term durability in switching operations.

To regulate humidity inside the chamber, a cooling system based on a Peltier cell is used. This system consists of a thermoelectric cooler, a radiator, and a fan. The Peltier cell cools the air circulating through the chamber. As the air cools, it condenses on the cold surfaces inside the dryer. This process effectively removes the water vapor produced by the mice, which helps maintain a stable relative humidity. The cooled and dehumidified air is then returned to the chamber.

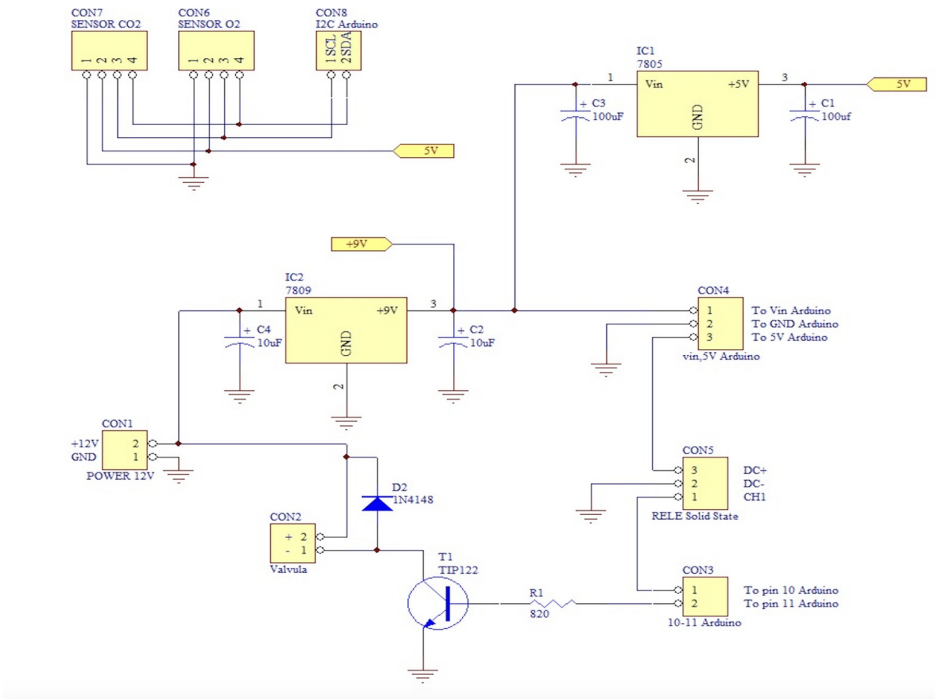


Figure 4. Schematic.

### 5.5. Arduino Control

The Arduino firmware is structured to manage real-time acquisition, display, control, and recording of oxygen (O<sub>2</sub>) and carbon dioxide (CO<sub>2</sub>) concentrations, along with temperature and relative humidity. These values are periodically sampled and visualized on a 3.5" TFT LCD driven by the TFT\_HX8357 library. Upon initialization, communication with all peripherals is established via I<sup>2</sup>C and SPI interfaces. A graphical interface is then rendered on the display, including axes for time and gas concentration, grid lines, and fixed legends for the visual interpretation of data. A rectangular plotting area is drawn for graphing real-time measurements. Initial error checks are performed to verify sensor integrity. The main function of the code contains the core operational logic and it is executed iteratively. At each iteration, the system checks whether new data is available from the CO<sub>2</sub> sensor. In the event of a sensor error (basically checked by the I<sup>2</sup>C bus), the nitrogen solenoid valve is closed and the air pump is activated, so animals are subjected to room air until the error is fixed. Once valid data are retrieved, the CO<sub>2</sub> concentration, temperature, and humidity values are

updated. Simultaneously, the O<sub>2</sub> sensor performs an averaged measurement based on ten samples, providing a smoothed value of the ambient oxygen concentration. The numerical values of humidity, temperature, CO<sub>2</sub>, and O<sub>2</sub> are updated on the display interface every 3–5 seconds, in accordance with the conversion time of the CO<sub>2</sub> and O<sub>2</sub> sensors. Approximately every 7 minutes, the system plots instantaneous values of O<sub>2</sub> and CO<sub>2</sub> on a dynamic scrolling graph. The X-axis represents time (scaled to cover 48 hours with 412 data points), while the Y1 and Y2 axes are scaled to appropriately display O<sub>2</sub> (%) and CO<sub>2</sub> (ppm) concentrations, respectively. A circular buffer mechanism ensures efficient redrawing of the graph without overloading memory. Figure 5 shows the graphical interface on the display. Simultaneously, the system logs environmental data to an SD card every 60 seconds, including timestamp, temperature, humidity, O<sub>2</sub> concentration, and CO<sub>2</sub> concentration. This allows for offline analysis and long-term monitoring.

A bang-bang controller is used to maintain the gas mixture at the desired values during the experiments. On the one hand, if the oxygen concentration exceeds the setpoint (11% in the examples), the system activates the N<sub>2</sub> valve until the level reaches the setpoint. Once this setpoint value is reached, the valve is deactivated, cutting off the N<sub>2</sub> supply. On the other hand, if the O<sub>2</sub> level drops below a critical value (setpoint-0.5% in the examples), or the CO<sub>2</sub> concentration exceeds a critical value (2000 ppm), the N<sub>2</sub> valve is automatically closed, and a room air (i.e., oxygenation) pump is activated until the O<sub>2</sub> / CO<sub>2</sub> levels are restored to the defined setpoints (11% and 1500 ppm respectively). Depending on the specific experiment aim, if the 2000 ppm threshold is considered too high, it can be lowered by simply modifying its value in the code.

The choice for bang-bang control is made, apart from being simple to implement, because this type of controller offers faster spin up times. This is especially important in applications where the system needs to be frequently manipulated (long periods with the door open or the equipment switched off). Nevertheless, it is well-known that bang-bang controllers present two main drawbacks, which could lead to experimental problems if very precise FiO<sub>2</sub> is required: ripple in the signal and risk of overdamping. As is shown in the next section, we have not observed overdamping, and the ripple is within acceptable range for most applications. If more precision is required to mimic certain pathologies, we advise implementing a more complex control scheme, such as proportional-integral-derivative (PID). It should be noted that, however, the PID parameters are more difficult to tune, so the intervention of technical personnel will be needed whenever any of the experimental parameters are changed (number of animals, gas pressures, etc.)

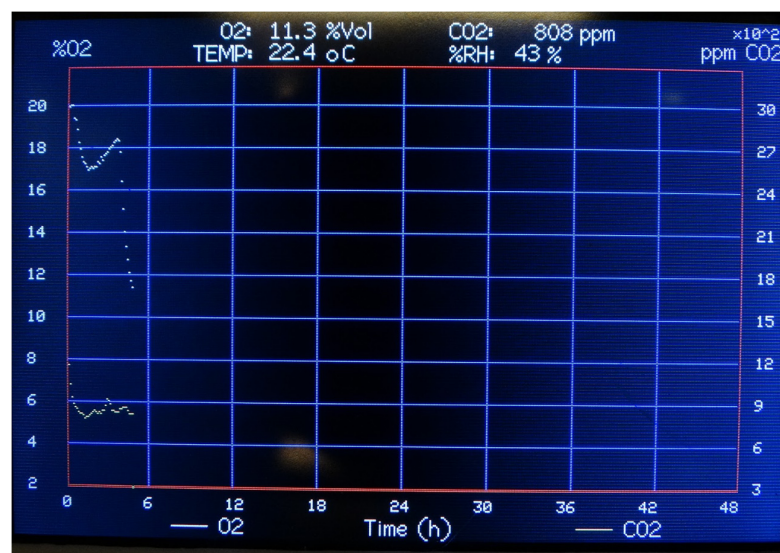


**Figure 5.** The graphical interface on the display. This example shows the first 5 h of a recording where the N<sub>2</sub> source functioning was intentionally altered to more clearly observe sudden changes in O<sub>2</sub> concentration.

## 6. Operation Instructions

Starting application of chronic hypoxia to mice requires the following initial actions: connecting the device to an electrical power line (preferably with backup), placing a recipient at the outlet tube of the Peltier-based air conditioning unit to collect the condensed water, filling the soda lime containers, connecting the device N<sub>2</sub> inlet to a pressured source (e.g., a cylinder), setting its low pressure/flow regulator to provide a N<sub>2</sub> flow able to reduce the chamber O<sub>2</sub> concentration from room air (21%) to the 11% set point in 10-20 min, place the animal cages into the chamber, carefully closing the windows and pressing the power on button.

During application of continuous hypoxia, the real time values of O<sub>2</sub> and CO<sub>2</sub> concentrations, temperature and relative humidity within the chamber can be seen in the front panel of the control unit. The screen in the front panel shows an updated time course of O<sub>2</sub> and CO<sub>2</sub> concentrations for the last 48 h (e.g., allowing checking that the system has worked correctly along an unattended weekend). The most important maintenance task is to replace the soda lime when required (either because it starts changing color from white to blue or because CO<sub>2</sub> concentration starts to increase above desired values). When a mice cage is extracted from the chamber (either for cleaning, feeding replacement or for animal examination), the window must be closed immediately to minimize gas concentration changes into the chamber. Users should be aware of the information provided by the sensors technical data sheets regarding periodic calibration checking and sensors lifelong.

For simplicity and taking into account that the process of reducing O<sub>2</sub> from room air (21%) to the chronic hypoxic target (11%) only occurs once at the beginning of the experiment, we did not include an automatically controlled time-course for the O<sub>2</sub> reduction. This initial process of animal adaptation should be carried out under the direct supervision of the investigator, and he/she can manually modulate the rate of hypoxia application by partially opening one of the box door's. However, it would be easy to include a very few sentences in the code to limit the rate of O<sub>2</sub> concentration reduction.

In case the device is used at conditions involving high air humidity and halogenated anesthetics, it is advisable to include a CO sensor [16,17]. In this work we have quantified the O<sub>2</sub> concentration by its percentage in air, as is it more usual by assuming working at sea level. However, in case the chamber is used in high altitude places where atmospheric pressure is below that of sea level, it should be taken into consideration that the physiologically relevant variable for O<sub>2</sub> concentration is its partial pressure.

## 7. Validation and Characterization

The passive dynamic change in gas concentration depends on both the chamber volume and the flow of gas leakage between the chamber and the room. We first characterized the passive time constant of gas concentration change in the chamber by measuring the O<sub>2</sub> concentration when the provision of N<sub>2</sub> was purposely interrupted when the chamber was at a stable 11% O<sub>2</sub> concentration. Figure 6 shows an exponential variation corresponding to a time constant ( $\tau$ ) of 3.34 h.

The in vivo performance of the device was validated when applying it in research studies where mice were experiencing chronic hypoxia. Figure 7 shows an example of the O<sub>2</sub> and CO<sub>2</sub> concentrations, temperature and relative humidity signals recorded when 17 wild-type mice were subjected to 11% O<sub>2</sub>. Data in the figure starts when the mice were initially introduced into the hypoxia chamber at conventional lab ambient conditions and hypoxia application was initiated. As expected, O<sub>2</sub> concentration decreased from lab conditions (21%) to the 11% set point and subsequently remained stable at this value with negligible oscillations (10.8–11.2%). CO<sub>2</sub> absorption was very effective since its concentration was reduced from the initial room lab value  $\approx$ 1000 ppm; i.e., 0.1%) to  $\approx$ 800 ppm, showing a considerable reserve capacity of the device to keep safe levels of CO<sub>2</sub> concentration. The figure also shows that, after a very minor initial fluctuation resulting from the sudden N<sub>2</sub> injection to lower O<sub>2</sub> concentration until the set point, ambient temperature and relative

humidity in the hypoxia chamber were maintained at values very close to the external lab room air  $\approx 45\%$  and  $\approx 22^{\circ}\text{C}$ , respectively.  $\text{N}_2$  consumption to keep the 11%- $\text{O}_2$  state steady was only  $\approx 2 \text{ l/min}$ .

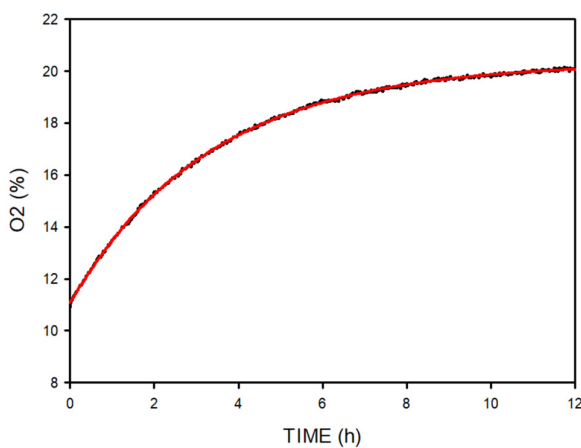


**Figure 6.** Time constant of gas exchange in the chamber. Passive change in chamber  $\text{O}_2$  concentration from stable 11%  $\text{O}_2$  after the  $\text{N}_2$  provision was interrupted. The black line is recorded data, and the red line is the exponential fitting with time constant  $\tau$ .

Uniform distribution of  $\text{CO}_2$  concentration within the chamber was confirmed by measuring it when the 19 mice were maintained under steady state condition. Indeed, by placing a  $\text{CO}_2$  sensor at the 9 different chamber sites potentially occupied by the mice cages, we observed that the variability (coefficient of variation) in the  $\text{CO}_2$  concentration within the chamber was only 6%.

These validation data and the suitability of the corresponding setting parameters correspond to the specific device built and animals employed. Users should adapt the device parameters, and validate them, in case of different applications, mainly depending on the number of animals and their metabolic rate (i.e.,  $\text{O}_2$  consumption).

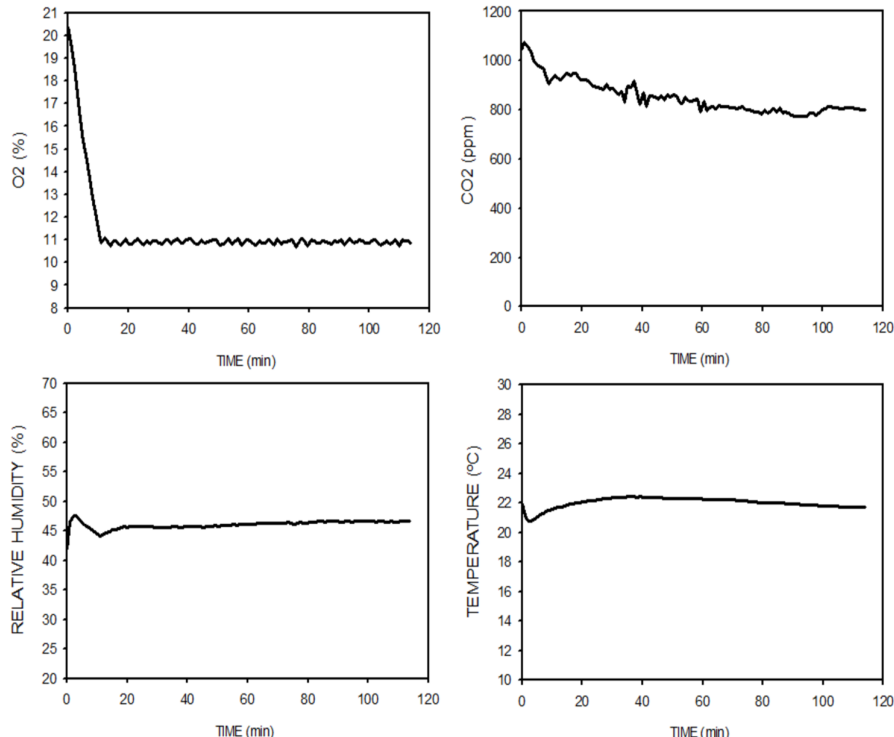


**Figure 7.** Example of the signals recorded inside the hypoxic chamber when subjecting mice to 11% chronic hypoxia from initial lab air conditions.

The maneuver consisting of opening a box door, taking out a mice cage and closing the door again (e.g., for cleaning and checking the animals) minimally disturbs the O<sub>2</sub> concentration within the box. Indeed, data from repeated measurements when the box was at a stable 11% O<sub>2</sub> concentration with the 17 mice inside resulted in a maximum O<sub>2</sub> concentration increased to 11.8%±0.1% (mean±SD) 65±9 s after ending the maneuver, and O<sub>2</sub> concentration automatically recovered the 11% steady state value 67±12 s after the transient maximum increase. Thus, O<sub>2</sub> concentration was altered by less than 1% for just 2 min.

**Ethics statements:** The mice experimental procedure was approved by the Ethical Committee for Animal Research of the Vall d'Hebrón Research Institute of Barcelona (approval number 51/24).

**CRediT author statement:** **Jorge Otero:** Technical conceptualization, Methodology, Writing-Reviewing; **Daniel Mbanze:** Methodology; **Miguel A. Rodríguez-Lázaro:** Methodology, Validation; **Raffaella Salama:** Methodology, Writing; **Gorka Solana:** Methodology; **Vicent Muñoz-Vaño:** Animal model testing; **Yolanda Cámara:** Animal model testing; **Isaac Almendros:** Animal model testing; **Ramon Farré:** General conceptualization, Methodology, Validation, Writing-Reviewing, Editing, and Supervision.

**Acknowledgments:** This work was partially funded by the Spanish Ministry of Science, Innovation and Universities (project reference: PID2023-147668OB-I00).

## References

1. GBD Chronic Respiratory Disease Collaborators. Prevalence and attributable health burden of chronic respiratory diseases, 1990-2017: a systematic analysis for the Global Burden of Disease Study 2017. Lancet Respir Med. 2020 Jun;8(6):585-596. doi: 10.1016/S2213-2600(20)30105-3.
2. Mensah, G, Fuster, V, Murray, C. et al. Global Burden of Cardiovascular Diseases and Risks, 1990-2022. JACC. 2023 Dec, 82 (25) 2350–2473. <https://doi.org/10.1016/j.jacc.2023.11.007>.
3. Powell-Wiley TM, Poirier P, Burke LE, Després JP, Gordon-Larsen P, Lavie CJ, Lear SA, Ndumele CE, Neeland IJ, Sanders P, St-Onge MP; American Heart Association Council on Lifestyle and Cardiometabolic Health; Council on Cardiovascular and Stroke Nursing; Council on Clinical Cardiology; Council on Epidemiology and Prevention; and Stroke Council. Obesity and Cardiovascular Disease: A Scientific Statement From the American Heart Association. Circulation. 2021 May 25;143(21):e984-e1010. doi: 10.1161/CIR.0000000000000973.
4. Shah NM, Kaltsakas G. Respiratory complications of obesity: from early changes to respiratory failure. Breathe (Sheff). 2023 Mar;19(1):220263. doi: 10.1183/20734735.0263-2022.
5. Zhao D, Wang Y, Wong ND, Wang J. Impact of Aging on Cardiovascular Diseases: From Chronological Observation to Biological Insights: JACC Family Series. JACC Asia. 2024 Apr 8;4(5):345-358. doi: 10.1016/j.jacasi.2024.02.002.
6. Cho SJ, Stout-Delgado HW. Aging and Lung Disease. Annu Rev Physiol. 2020 Feb 10;82:433-459. doi: 10.1146/annurev-physiol-021119-034610.
7. Chen, PS., Chiu, WT., Hsu, PL. et al. Pathophysiological implications of hypoxia in human diseases. J Biomed Sci 27, 63 (2020). <https://doi.org/10.1186/s12929-020-00658-7>.
8. Ortmann BM, Taylor CT, Rocha S. Hypoxia research, where to now? Trends Biochem Sci. 2024 Jul;49(7):573-582. doi: 10.1016/j.tibs.2024.03.008.
9. Hillman TC, Idnani R, Wilson CG. An Inexpensive Open-Source Chamber for Controlled Hypoxia/Hyperoxia Exposure. Front Physiol. 2022 Jul 12;13:891005. doi: 10.3389/fphys.2022.891005.
10. Ferrari M, Jain IH, Goldberger O, Rezoagli E, Thoonen R, Cheng KH, Sosnovik DE, Scherrer-Crosbie M, Mootha VK, Zapol WM. Hypoxia treatment reverses neurodegenerative disease in a mouse model of Leigh syndrome. Proc Natl Acad Sci U S A. 2017 May 23;114(21):E4241-E4250. doi: 10.1073/pnas.1621511114.

11. Kim, E. R., and Tong, Q. (2017). Oxygen consumption rate and energy expenditure in mice: indirect calorimetry. *Methods Mol. Biol.* 1566, 135–143. doi:10.1007/978-1-4939-6820-6\_13.
12. Olesen, B. W., Bogatu, D.-I., Kazanci, O., and Coakley, D. (2021). The use of CO<sub>2</sub> as an indicator for indoor air quality and control of ventilation according to EN16798-1 and TR16798-2. Paper presented at 15th ROOMVENT Conference Available at: <https://orbit.dtu.dk/en/publications/the-use-of-cosub2sub-as-an-indicator-for-indoor-airquality-and-c>.
13. Hirabayashi G, Uchino H, Sagara T, Kakinuma T, Ogihara Y, Ishii N. Effects of temperature gradient correction of carbon dioxide absorbent on carbon dioxide absorption. *Br J Anaesth.* 2006 Oct;97(4):571-5. doi: 10.1093/bja/ael210.
14. Fairchild GA. Measurement of respiratory volume for virus retention studies in mice. *Appl Microbiol.* 1972 Nov;24(5):812-8. doi: 10.1128/am.24.5.812-818.1972.
15. Haines H, Shield CF, Twitchell C. Reduced evaporation from rodents during prolonged water restriction. *Life Sciences*, Volume 8, Issue 19, Part 1, 1969, Pages 1063-1068. [https://doi.org/10.1016/0024-3205\(69\)90158-1](https://doi.org/10.1016/0024-3205(69)90158-1).
16. Fang ZX, Eger EI 2nd, Lesser MJ, Chortkoff BS, Kandel L, Ionescu P. Carbon monoxide production from degradation of desflurane, enflurane, isoflurane, halothane, and sevoflurane by soda lime and Baralyme. *Anesth Analg.* 1995 Jun;80(6):1187-93. doi: 10.1097/00000539-199506000-00021.
17. Keijzer, C., Perez, R.S. & De Lange, J.J. Carbon monoxide production from five volatile anesthetics in dry sodalime in a patient model: halothane and sevoflurane do produce carbon monoxide; temperature is a poor predictor of carbon monoxide production. *BMC Anesthesiol* 5, 6 (2005). <https://doi.org/10.1186/1471-2253-5-6>.

**Disclaimer/Publisher's Note:** The statements, opinions and data contained in all publications are solely those of the individual author(s) and contributor(s) and not of MDPI and/or the editor(s). MDPI and/or the editor(s) disclaim responsibility for any injury to people or property resulting from any ideas, methods, instructions or products referred to in the content.